

基于宽、窄带和频法的超辐射光三倍频仿真

章旭^{1,2}, 季来林², 刘栋², 高妍琦², 隋展², 赵晓晖^{2*}, 向霞^{1*}¹电子科技大学物理学院, 四川 成都 611731;²中国工程物理研究院上海激光等离子体研究所, 上海 201800

摘要 高效宽带的三次谐波转换是激光惯性约束聚变驱动器的关键技术之一。超辐射光的宽带特性以及宽、窄带和频方案为这一研究提供了新的实现途径。本文基于超辐射光特性,建立了其三倍频过程数值计算模型,并分析了时间高相干基频光与超辐射倍频光和频的效率和光谱特性演化。与超辐射光直接三倍频相比,宽、窄和频方案能够有效地减小群速度失配对超辐射光三倍频效率的影响,可以将超辐射光三倍频效率提升至 44%,输出三倍频带宽可达到 1.9 THz,该结果可指导超辐射光三倍频系统的设计与相关实验研究。

关键词 非线性光学; 超辐射光; 非线性频率转换; 群速度失配

中图分类号 O437

文献标志码 A

doi: 10.3788/CJL202148.2108001

1 引言

在激光驱动惯性约束聚变(ICF)研究中,一般采用钕玻璃激光三倍频(351 nm)打靶,以有效地提高激光与等离子体的耦合效率^[1-3],同时进一步增加激光相对带宽($\Delta\nu/\nu$)至 1%左右,可有效抑制激光与等离子体相互作用过程中不稳定性的增长,减少后向受激散射和超热电子的产生^[4-5],但由于光场高速调制技术、高增益放大过程增益窄化和高效三倍频带宽窄等原因,目前激光驱动器的输出带宽不大于 0.3 nm (100 GHz)。低相干光的用途广泛,可用于测距^[6]或相位恢复^[7],而为了解决物理实验中的不稳定性等问题,宽带低相干激光在 ICF 的应用受到了关注^[8-9]。近期,中国工程物理研究院上海激光等离子体研究所成功研制基于超辐射光放大的时间低相干激光系统,可获得带宽 12 nm,脉冲宽度 3 ns,能量 1 kJ 的基频(FW)时间低相干脉冲输出^[10-11],相比于现役驱动器输出带宽提升了 1~2 个数量级,并采用低掺氘 DKDP 晶体,成功实现了 70%的倍频效率^[12],并有望将该方案移植于现役驱动器装置中。

如前所述,ICF 物理研究更倾向于三倍频,超辐

射光如能实现高效三倍频,将会为该方案的工程应用提供更坚实基础,但现有非线性晶体无法同时满足三倍频过程(THG)的相位匹配与群速度匹配,高效三倍频过程的基频接收带宽不超过 0.3 nm (100 GHz)。针对这一难题,国内外提出了多种解决方案,例如光谱角色散补偿^[13-14]、啁啾调控匹配^[15-16]、晶体级联^[17-18]、折返点匹配^[19]以及宽、窄带和频^[20]等方法。

上述方法中,采用光谱角色散补偿方案,将在光路内插入大量元件,增大了光路损耗以及调节的复杂性,且只补偿了相位失配线性项,当带宽变大或脉冲的啁啾率增加时,相位失配展开的二次项会变大,该方法很难完全补偿相位失配。啁啾调控匹配方案同样面临光路复杂、元件易损伤等问题,并且产生的三倍频光束仍是线性啁啾脉冲,不能很好满足物理实验要求。晶体级联方法虽然光路简单,但没有真正解决群速度失配的问题,高效三倍频过程的基频接收带宽不大于 1 nm (270 GHz)。折返点匹配法原理虽然简单,但依赖于新的可用晶体材料的发明,目前尚未发现合适的非线性晶体。而宽、窄带和频方法可将三倍频过程中群速度失配的影响减小至原来的 $2/7$ ^[21],将有效提升三倍频带宽,且光路插入元

收稿日期: 2021-03-24; 修回日期: 2021-04-12; 录用日期: 2021-04-21

基金项目: 国家自然科学基金(11804321, 12074353)、科学挑战计划(TZ2016005)

通信作者: *xiaxiang@uestc.edu.cn; **xhzhao_silp@163.com

件少,具有较大的工程应用价值,将该方案应用于超辐射光放大的时间低相干激光系统,有望改善其三倍频转换效率。

本文建立了超辐射光三倍频过程的数值计算模型,分析了基于宽、窄带和频方法提升超辐射光脉冲三倍频效率的效果,经过参数优化,实现了 44% 三倍频转换效率,输出三倍频带宽可达到 0.78 nm (1.9 THz)。

2 基于宽、窄带和频方案的三倍频过程仿真与分析

在频率转换过程中,存在着群速度失配量(默认三波关系满足 $\omega_1 = \omega_2/2 = \omega_3/3$),

$$\left(\frac{d\Delta k}{d\omega_1}\right)\Bigg|_{\omega_0} \Delta\omega = \left(\frac{dk_3}{d\omega_1} - \frac{dk_2}{d\omega_1} - \frac{dk_1}{d\omega_1}\right)\Bigg|_{\omega_0} \Delta\omega = \left(3\frac{1}{v_{g3}} - 2\frac{1}{v_{g2}} - \frac{1}{v_{g1}}\right)\Delta\omega, \quad (1)$$

式中: k_i 表示各波波矢大小; ω_i 表示各波的频率; v_{gi} 表示各波的群速度。可知,群速度失配与入射带宽成正比,当没有补偿频率转换过程中失配量时,随着入射带宽的增大,频率转换的效率与带宽都会随之下降。

宽、窄带和频方案利用宽带光与窄带光进行和频,可减小群速度失配对和频过程的影响,Zhao 等^[22]采用 800 nm 的啁啾展宽脉冲与窄带 1053 nm 脉冲的和频,证实了该方法的有效性。Chen 等^[20-21]指出三倍频与基频之间的群速度失配约为三倍频与倍频之间的群速度失配的 5 倍且前者引起的波矢失配量约为群速度失配引起的波矢失配量的 5/7,并提出了使用窄带基频脉冲与另一束啁啾展宽倍频脉冲和频的方案,使与窄带相关的三倍频与基频之间

的群速度失配不起作用。但是啁啾展宽的脉冲难以满足物理实验的需求,只有当激光为连续谱或光谱相位随机时才能得到预期的抑制效果^[23]。借鉴该方法,使用高相干的 1053 nm 窄带脉冲作为基频光,与超辐射倍频光进行和频,以提高超辐射光三倍频的转换效率,更好满足物理实验的需求。

在仿真过程中,超辐射光首先经过晶体倍频(SHG),再与窄带基频光在三倍频晶体中和频,进而得到三倍频光,如图 1 所示。

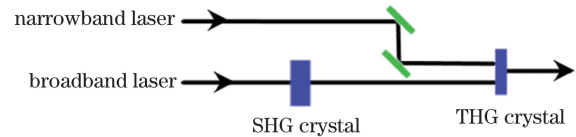


图 1 基于宽、窄带和频方案的三倍频过程示意图
Fig. 1 Schematic diagram of THG based on mixing broadband and narrowband

超辐射光场近似于混沌光,不具有解析形式,其功率谱接近均匀分布,类似于白噪声。根据文献^[24-25],先在频域中构建一个相位随机的白噪声电场,再通过傅里叶逆变换转换到时域中,进行脉冲整形得到对应的脉冲宽度,再回到频域中通过滤波函数获得所需要的光谱宽度。最后在时域中利用信号时间上的强度积分等于信号的平均强度,得到对应的时域分布。为了方便本文中三倍频过程的数值模拟结果的对比,以及与今后实验中由示波器和光谱仪采集的时间、频谱波形进行对照,对仿真得到的时域采用低通滤波,对频域采用移动均值滤波,如图 2 所示,图 2(a)为模拟所得的时间波形,图 2(b)为频域谱。

对于非线性转换过程,Armstrong 等^[26]利用量子理论详细分析了晶体中二、三次谐波转换机理后,

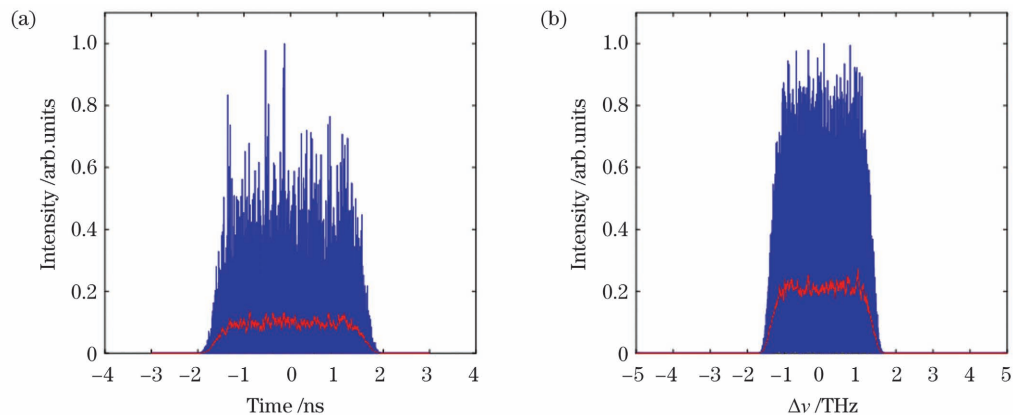


图 2 超辐射光的数值模型。(a)时域谱;(b)频域谱

Fig. 2 Numerical model of super-luminescent light. (a) Time domain spectrum; (b) frequency domain spectrum

经过多年的发展,谐波转换理论模型逐渐完善,将空间走离、群速度失配等空域、时域效应的影响囊括在内^[27-29]。由于超辐射光具有时间低相干、空间高相干的特性,因此,时域的走离效应(即群速度失配及群速度色散)将是影响其非线性频率转换过程的主要因素,而空域的效应可以忽略。简化后超辐射光的三倍频耦合波方程如下,

$$\frac{\partial A_1(z,t)}{\partial z} = -\frac{\alpha_1}{2}A_1(z,t) - \frac{1}{v_{g1}} \frac{\partial A_1(z,t)}{\partial t} - \frac{i}{2}\beta_1 \frac{\partial^2 A_1(z,t)}{\partial t^2} + i\kappa A_3 A_2^* \exp(i\Delta k z), \quad (2)$$

$$\frac{\partial A_2(z,t)}{\partial z} = -\frac{\alpha_2}{2}A_2(z,t) - \frac{1}{v_{g2}} \frac{\partial A_2(z,t)}{\partial t} - \frac{i}{2}\beta_2 \frac{\partial^2 A_2(z,t)}{\partial t^2} + i2\kappa A_3 A_1^* \exp(i\Delta k z), \quad (3)$$

$$\frac{\partial A_3(z,t)}{\partial z} = -\frac{\alpha_3}{2}A_3(z,t) - \frac{1}{v_{g3}} \frac{\partial A_3(z,t)}{\partial t} - \frac{i}{2}\beta_3 \frac{\partial^2 A_3(z,t)}{\partial t^2} + i3\kappa A_1 A_2 \exp(-i\Delta k z), \quad (4)$$

式中: A 表示光的复振幅; α 为在晶体中的吸收系数; β_i 表示各波在晶体中的群速度色散; κ 为耦合系数; Δk 为中心频率的波矢失配量; z 表示波矢的传播方向。

仿真过程中,放大的超辐射光的脉冲宽度为 3.5 ns,并根据不同的方案,其频率宽度分别为 3 THz、2 THz、1 THz。窄带基频输入为波长 1053 nm 的单色光,脉冲形状为宽度 3.5 ns 的单体 10 阶超高斯脉冲。基频的吸收系数 $\alpha_1 = 0.058 \text{ cm}^{-1}$,倍频吸收系数 $\alpha_2 = 0.058 \text{ cm}^{-1}$,三倍频吸收系数 $\alpha_3 = 0.008 \text{ cm}^{-1}$,倍频过程耦合系数为 $\kappa_1 = 0.8356 \times 10^{-6}$,三倍频过程的耦合系数为 $\kappa_2 = 1.0837 \times 10^{-6}$ 。倍频晶体采用 15% 掺铀率的 DKDP,三倍频晶体为 KDP 晶体,且满足 I/II 类匹配过程,皆满足中心波长 1053 nm 处的相位匹配。各波在二倍频过程以及三倍频过程中的中心频率的群速度与群速色散如表 1 所示。

2.1 倍频、三倍频晶体厚度的优化

对于谐波转换过程,薄晶体能够提高转换带宽,但晶体过薄则会限制转换效率,而晶体过厚则会使谐波转换过程发生能量的“倒流”现象。因此,针对中心波长 1053 nm,带宽 3 THz (11.08 nm),脉冲宽度 3.5 ns 的超辐射光基频输入,进行倍频晶体以及三倍频晶体的厚度的优化,以获得理论上的三倍频最高转换效率。

表 1 非线性晶体中的群速度与群速色散

Table 1 Group velocity and group velocity dispersion in nonlinear crystal

Waves in harmonic-generation	$U_g^{-1}/$ ($10^{-9} \text{ s} \cdot \text{m}^{-1}$)	$\beta /$ ($10^{-27} \text{ s}^2 \cdot \text{m}^{-1}$)
1 ω in SHG	5.0757	-8.47
2 ω in SHG	5.0744	70.23
1 ω in THG	4.9506	11.11
2 ω in THG	5.1505	72.38
3 ω in THG	5.1985	126.78

宽、窄带和频过程中的基频能量是额外引入的,而非倍频过程中的剩余基频,因此需控制窄带基频的能量输入,使基频与倍频的光子数之比约为 1:1。

在较高的光强条件下(2~3 GW/cm²),超辐射光能够实现约 80% 的倍频效率^[6]。一般高功率激光驱动器输出基频光强在 1~3 GW/cm²,频率转换系统设计,需要兼顾转换效率与基频光强的动态范围,从而选择合理的晶体厚度。对于宽、窄带和频方案的三倍频转换效率(η)的计算方式为

$$\eta = \frac{I_{\text{THG}}}{I_{\text{SLD}} + I_{\text{Gauss}}}, \quad (5)$$

式中: I_{THG} 表示频率转换过程得到的三倍频的光强; I_{SLD} 为超辐射宽带光入射光强; I_{Gauss} 则为窄带光入射光强。

计算发现,当倍频晶体长度为 19 mm 时,能够使基频光强在 2~3 GW/cm² 的范围内得到较为稳定且高效的倍频转换效率,此时倍频转换效率约为 84.3%,具体如图 3(a)所示。因此将窄带基频光能量与超辐射脉冲能量的比例设置为 0.843:2,可使和频过程中基频与倍频的光子数之比接近 1:1。选取 6 mm 厚的和频 KDP 晶体,对应的三倍频转换效率可高达 44%,如图 3(b)所示。

图 3(c)为经过优化后,对应的超辐射基频光谱、倍频光谱以及宽、窄带和频后的三倍频光谱,坐标已做归一化。由于超辐射光相位随机的特性,使得倍频过程不仅为各个频谱成分自身的倍频,而且还包含频率之间的和频,根据统计光学与维纳-欣钦定理可得超辐射光对应的倍频频谱强度是基频频谱的自卷积结果^[7]。在倍频的模拟仿真过程中,基频输入为带宽 3 THz,得到倍频带宽为 2.9 THz,其频谱形状近似为三角形,如图 3(c)所示,基本符合自卷积过程的理论预期。

而基于宽、窄带和频方案的三倍频过程得到的

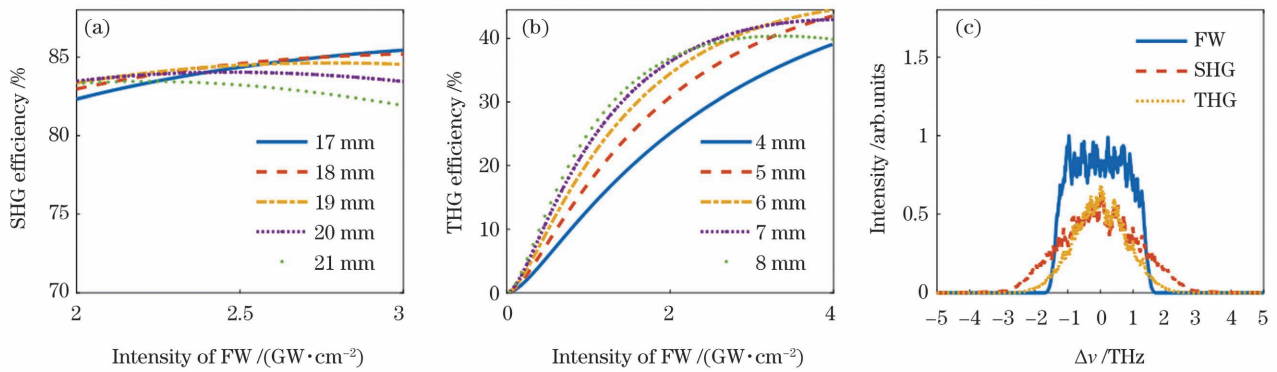


图 3 谐波转换过程的效率以及频谱。(a)晶体长度对倍频效率曲线的影响;(b)晶体长度对三倍频效率曲线的影响;(c)频率转换过程中各波的频谱

Fig. 3 Efficiency and spectra of harmonic generation. (a) Influence of crystal length on SHG efficiency curve; (b) influence of crystal length on THG efficiency curve; (c) spectrum of each wave in frequency conversion

三倍频频谱宽度为 1.9 THz, 相较倍频有所变窄, 主要原因在于三倍频过程的色散所导致的相位失配难以消除, 对于偏离中心波长的和频过程, 失配量的影响也会逐渐变大, 从而使光谱边缘的转换效率下降。

2.2 与超辐射脉冲直接三倍频的对比

确认了 3 THz 超辐射光宽带基频输入的宽、窄带和频方案的两块非线性晶体最佳厚度后, 进一步比较了宽带倍频与窄带基频的和频以及超辐射脉冲直接三倍频的模拟结果。其仿真结果如图 4 所示, 其中图 4(a) 为效率随超辐射脉冲光强变化曲线, 图 4(b)~(c) 分别为宽、窄带和频与超辐射脉冲直接三倍频的光谱。

对于超辐射光直接三倍频过程, 由于群速度失配的影响与带宽成正比。通过引入窄带作为三倍频过程中的基频光, 使得群速度失配中三倍频与基频之间的群速度失配失效, 群速度失配对三倍频过程

的影响减小至原来的 $2/7$, 从而使得光强范围 $3 \sim 4 \text{ GW/cm}^2$ 内三倍频的最高效率从 5% 提升至 44%, 如图 4(a) 所示。

此外, 图 4(b)~(c) 分别展示了宽、窄带和频方案以及宽带直接三倍频过程中各宽带光的频谱(图中的各波频谱根据宽带倍频输入最大强度归一化)。从图 4(b) 中看出, 在宽带超辐射脉冲与窄带基频的和频过程中, 由于窄带的引入(未在图中给出), 超辐射宽带脉冲的中心频率附近成分都有效参与了和频过程, 使得其三倍频中心频率处的最高光强超过了倍频光强。但其边带效率有所降低, 得到的三倍频频谱宽度约为 1.9 THz。宽带直接三倍频过程中, 因群速度失配完全没有得到补偿, 使得在整个频域上的三倍频转换效率都非常低, 由图 4(c) 可见。对比可知, 宽、窄带和频过程得到的三倍频输出的带宽相较于宽带直接三倍频有所变窄, 但效率得到了非常大的提升。

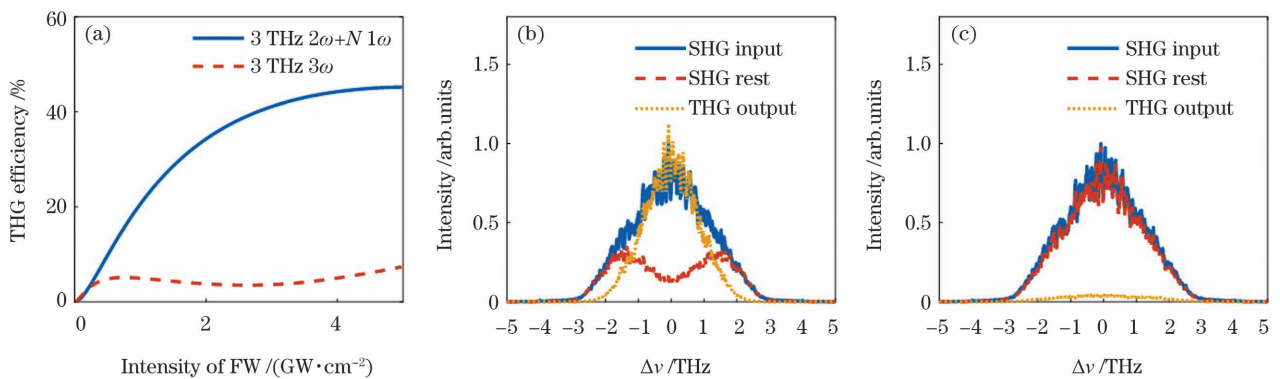


图 4 基于宽、窄带和频方案的三倍频过程与宽带直接三倍频的结果。(a)效率曲线;(b)宽带倍频(3 THz)与窄带基频和频的频谱;(c)宽带直接三倍频的频谱

Fig. 4 THG results of mixing broadband and narrowband and direct THG. (a) Efficiency curves; (b) spectrum of mixing broadband SHG (3 THz) and narrowband FW; (c) spectrum of direct THG

2.3 与不同输入的宽、窄带和频过程的对比

进一步对比分析超辐射光的入射带宽变化对宽带倍频与窄带基频的和频过程的影响,模拟结果如图 5 所示(图中的各波频谱根据宽带倍频输入最大强度归一化)。

图 5(a)为不同带宽的超辐射光对应的宽带倍频与窄带基频的和频过程的效率曲线,可以发现缩小了宽带基频输入的带宽后,效率只得到了小幅度的提升,并且 2 THz 和 1 THz 的宽带基频输入的宽、窄带和频过程的效率曲线在能量密度为 $4 \text{ GW}/\text{cm}^2$ 之前基本保持一致,最高效率大约

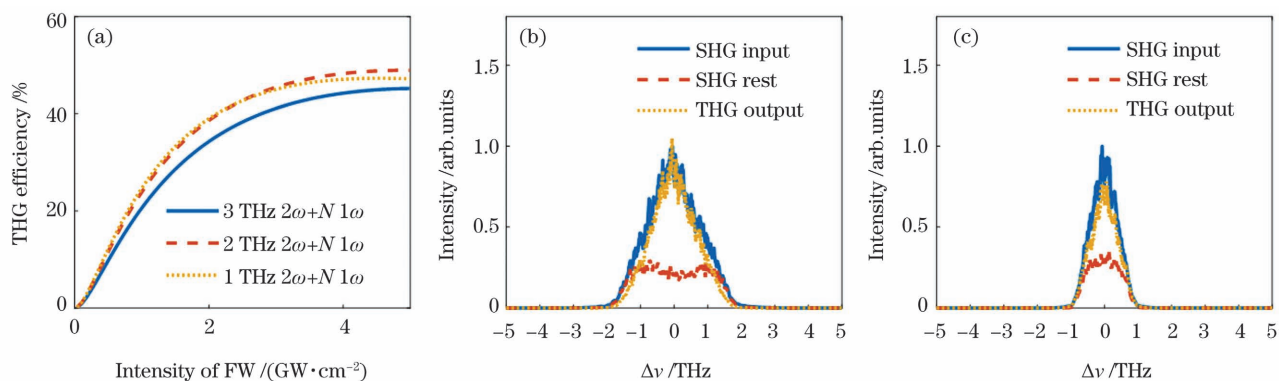


图 5 不同带宽输入的宽带倍频与窄带基频的和频过程结果。(a)效率曲线;(b)宽带倍频(2 THz)与窄带基频和频的频谱;(c)宽带倍频(1 THz)与窄带基频和频的频谱

Fig. 5 Results of different bandwidth of mixing broadband SHG and narrowband FW. (a) Efficiency curve; (b) spectrum of mixing broadband SHG (2 THz) and narrowband FW; (c) spectrum of mixing broadband SHG (1 THz) and narrowband FW

2.4 宽带基频与窄带倍频的和频过程

还对比了超辐射光宽带基频与窄带倍频和频的方案,在 $3\sim 4 \text{ GW}/\text{cm}^2$ 的范围内,其最高效率约为 17%。该方案消除了倍频光与三倍频光的群速度失配的影响,但其对三倍频过程的影响小于三倍频与基频之间的群速度失配,因此,该方案的转换效率高

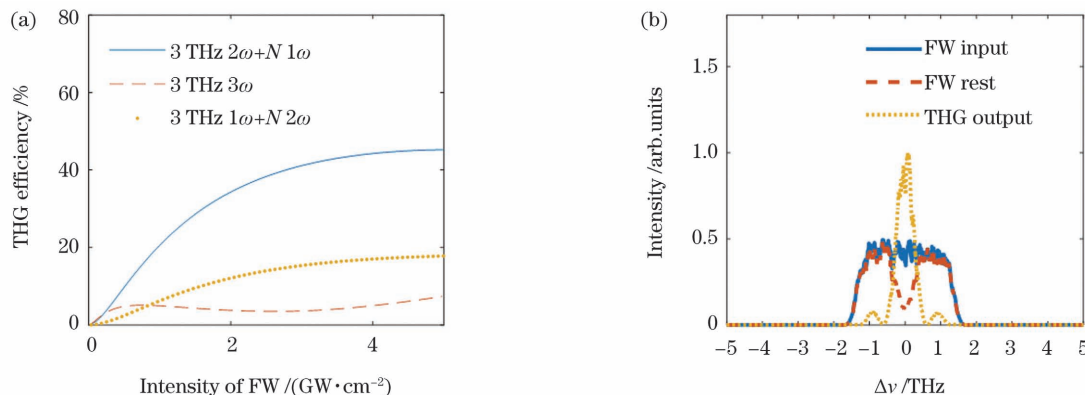


图 6 宽带基频与窄带倍频和频的仿真结果。(a)效率曲线;(b)宽带基频(3 THz)与窄带倍频和频过程中各波的频谱

Fig. 6 Results of mixing narrowband FW and broadband SHG. (a) Efficiency curve; (b) spectrum of mixing narrowband SHG and broadband FW (3 THz)

为 48%。

对于 3 THz、2 THz 和 1 THz 的宽带基频输入,其宽、窄带和频过程的输出带宽分别为 1.9 THz、1.7 THz 和 0.9 THz,并且 2 THz 和 1 THz 的宽带基频输入能在整个频谱范围上充分转换,得到与倍频输入基本一致的三倍频频谱波形,但随着倍频输入带宽的减小,所得到的三倍频的带宽也会随之减小,如图 5(b)~(c)所示。原因在于优化后晶体厚度为 6 mm,在 2 THz (2ω) 带宽内的相位失配量是非常有限的,不足以显著影响效率。若要继续增大三倍频带宽,则需要进一步补偿群速度失配。

于超辐射脉冲直接三倍频但低于宽带倍频与窄带基频和频。图 6(a)的效率曲线结果符合理论认知。

图 6(b)给出了宽带基频与窄带倍频和频过程中各宽带光的频谱波形(根据三倍频输出最大强度归一化)。从宽带基频输入与剩余的宽带基频的对比可看出,由于群速度失配量的影响,使得能够参与

三倍频的宽带基频范围有限,虽然中心频率附近得到较为充分的转换,但因为其影响相对较小,因此光谱边缘基本不参与三倍频过程,频谱宽度仅为 0.9 THz。

综上所述,在倍频晶体厚度 19 mm,三倍频晶体厚度 6 mm 的条件下,频谱宽度为 3 THz 的超辐射光直接三倍频的转换带宽约为 3 THz,转换效率仅为 5%。而采用超辐射光倍频与窄带基频和频的方案,能够实现频谱宽度约 1.9 THz,转换效率为 44%的三倍频输出。窄带倍频光与超辐射基频光和频的方案对群速度失配的补偿较小,其三倍频的转换带宽为 0.9 THz,转换效率为 17%。

3 结 论

本文建立了超辐射光三倍频过程的数值计算模型,模拟了超辐射倍频光与窄带基频光的三倍频过程,并对比分析了超辐射光直接三倍频和基于宽带超辐射倍频与窄带基频光和频的三倍频方案,证明了宽、窄带和频方案能够有效地减小超辐射光的三倍频过程中群速度失配,理论上可以显著提高转换效率,输出三倍频带宽接近 2 THz,转换效率大于 40%,相比超辐射光直接三倍频效率提高约 8 倍。这一研究为后续实现宽带高效的超辐射光三倍频过程的实验提供理论指导。

参 考 文 献

- [1] Slater D C, Busch G E, Charatis G, et al. Absorption and hot-electron production for 1.05 and 0.53 μm light on spherical targets [J]. *Physical Review Letters*, 1981, 46(18): 1199-1202.
- [2] Perkins L J, Betti R, LaFortune K N, et al. Shock ignition: a new approach to high gain inertial confinement fusion on the national ignition facility [J]. *Physical Review Letters*, 2009, 103 (4): 045004.
- [3] Lin W H, Zhu J Q, Ren L. Advances in target alignment and beam-target coupling technologies of laser fusion facility [J]. *Chinese Journal of Lasers*, 2020, 47(4): 0400001.
林炜恒, 朱健强, 任磊. 高功率激光装置中的靶定位及束靶耦合技术研究进展 [J]. *中国激光*, 2020, 47 (4): 0400001.
- [4] Skupsky S, Short R W, Kessler T, et al. Improved laser-beam uniformity using the angular dispersion of frequency-modulated light [J]. *Journal of Applied Physics*, 1989, 66(8): 3456-3462.
- [5] Rothenberg J E, Eimerl D, Key M H, et al. Illumination uniformity requirements for direct-drive inertial confinement fusion [J]. *Proceedings of SPIE*, 1995, 2633: 162-169.
- [6] Liu J Y, Lei F. Measurement of lens-center thickness based on low-coherence interference with transmitted illumination [J]. *Laser & Optoelectronics Progress*, 2019, 56(12): 121201.
刘经佑, 雷枫. 基于透过式低相干光学干涉测量透镜中心厚度 [J]. *激光与光电子学进展*, 2019, 56(12): 121201.
- [7] Lu X Y, Zhao C L, Cai Y J. Research progress on methods and applications for phase reconstruction under partially coherent illumination [J]. *Chinese Journal of Lasers*, 2020, 47(5): 0500016.
卢兴园, 赵承良, 蔡阳健. 部分相干照明下的相位恢复方法及应用研究进展 [J]. *中国激光*, 2020, 47 (5): 0500016.
- [8] Wei X F, Li P. Beam coherence and control of laser fusion driver: retrospect and prospect [J]. *High Power Laser and Particle Beams*, 2020, 32 (12): 121007.
魏晓峰, 李平. 激光聚变驱动器的光束相干性及其控制: 回顾与展望 [J]. *强激光与粒子束*, 2020, 32 (12): 121007.
- [9] Xu L H, Wang Y F, Jia Y F, et al. Research progress of low-coherence laser [J]. *Acta Optica Sinica*, 2021, 41(8): 0823008.
徐林海, 王宇飞, 贾宇飞, 等. 低相干性激光的研究进展 [J]. *光学学报*, 2021, 41(8): 0823008.
- [10] Gao Y Q, Ji L L, Cui Y, et al. kJ low-coherence broadband Nd: glass laser driver facility [J]. *High Power Laser and Particle Beams*, 2020, 32 (1): 011004.
高妍琦, 季来林, 崔勇, 等. kJ 级宽带低相干激光驱动装置 [J]. *强激光与粒子束*, 2020, 32(1): 011004.
- [11] Cui Y, Gao Y Q, Rao D X, et al. High-energy low-temporal-coherence instantaneous broadband pulse system [J]. *Optics Letters*, 2019, 44 (11): 2859-2862.
- [12] Ji L L, Zhao X H, Liu D, et al. High-efficiency second-harmonic generation of low-temporal-coherent light pulse [J]. *Optics Letters*, 2019, 44(17): 4359-4362.
- [13] Skeldon M D, Craxton R S, Kessler T, et al. Efficient harmonic generation with a broad-band laser [J]. *IEEE Journal of Quantum Electronics*, 1992, 28 (5): 1389-1399.
- [14] Pennington D M, Hennesian M A, Milam D, et al. Efficient broadband third-harmonic frequency conversion via angular dispersion [J]. *Proceedings of SPIE*, 1995, 2633: 645-654.

- [15] Osvey K, Ross I N. Efficient tuneable bandwidth frequency mixing using chirped pulses [J]. *Optics Communications*, 1999, 166 (1/2/3/4/5/6): 113-119.
- [16] Qian L J. Chirp matched third harmonic conversion for broad-band lasers[J]. *Acta Optica Sinica*, 1995, 15(6): 662-664.
钱列加. 宽频带激光的啁啾匹配型三次谐波转换[J]. *光学学报*, 1995, 15(6): 662-664.
- [17] Pronko M S, Lehmburg R H, Obenschain S, et al. Efficient second harmonic conversion of broad-band high-peak-power Nd: glass laser radiation using large-aperture KDP crystals in quadrature[J]. *IEEE Journal of Quantum Electronics*, 1990, 26(2): 337-347.
- [18] Ji L L, Zhu B Q, Liu C, et al. Optimization of quadrature frequency conversion with type-II KDP for second harmonic generation of the nanosecond chirp pulse at 1053 nm[J]. *Chinese Optics Letters*, 2014, 12(3): 031902.
- [19] Webb M S, Eimerl D, Velsko S P. Wavelength insensitive phase-matched second-harmonic generation in partially deuterated KDP[J]. *Journal of the Optical Society of America B*, 1992, 9(7): 1118-1127.
- [20] Chen Y, Yuan P, Qian L J, et al. Numerical study on the efficient generation of 351 nm broadband pulses by frequency mixing of broadband and narrowband Nd: glass lasers[J]. *Optics Communications*, 2010, 283(13): 2737-2741.
- [21] Chen Y. Efficient third-harmonic generation of broadband Nd: glass by frequency mixing of broadband and narrowband Nd: glass lasers[D]. Shanghai: Fudan University, 2010.
- 陈英. 高功率钕玻璃激光系统的宽带三倍频技术方案研究[D]. 上海: 复旦大学, 2010.
- [22] Zhao K, Yuan P, Zhong H Z, et al. Narrowband pulse-enhanced upconversion of chirped broadband pulses[J]. *Journal of Optics*, 2010, 12(3): 035206.
- [23] Follett R K, Shaw J G, Myatt J F, et al. Thresholds of absolute instabilities driven by a broadband laser [J]. *Physics of Plasmas*, 2019, 26(6): 062111.
- [24] Dorrer C. Statistical analysis of incoherent pulse shaping [J]. *Optics Express*, 2009, 17(5): 3341-3352.
- [25] Ji L L, Zhao X H, Liu D, et al. Research progress of low-temporal-coherence light frequency conversion technology for high power Nd: glass laser system [J]. *High Power Laser and Particle Beams*, 2020, 32(11): 112009.
季来林, 赵晓晖, 刘栋, 等. 高功率钕玻璃激光系统低时间相干光频率转换技术研究进展[J]. *强激光与粒子束*, 2020, 32(11): 112009.
- [26] Armstrong J A, Bloembergen N, Ducuing J, et al. Interactions between light waves in a nonlinear dielectric[J]. *Physical Review*, 1962, 127(6): 1918-1939.
- [27] Craxton R. High efficiency frequency tripling schemes for high-power Nd: glass lasers[J]. *IEEE Journal of Quantum Electronics*, 1981, 17(9): 1771-1782.
- [28] Auerbach J M, Eimerl D, Milam D, et al. Perturbation theory for electric-field amplitude and phase ripple transfer in frequency doubling and tripling[J]. *Applied Optics*, 1997, 36(3): 606-618.
- [29] Wegner P J, Hennesian M A, Speck D R, et al. Harmonic conversion of large-aperture 105 μm laser beams for inertial-confinement fusion research [J]. *Applied Optics*, 1992, 31(30): 6414-6426.

Numerical Simulation on Third-Harmonic Generation of Super-Luminescent Light by Mixing Broadband and Narrowband Lasers

Zhang Xu^{1,2}, Ji Lailin², Liu Dong², Gao Yanqi², Sui Zhan², Zhao Xiaohui^{2*}, Xiang Xia^{1*}

¹ School of Physics, University of Electronic Science and Technology of China, Chengdu, Sichuan 610054, China;

² Shanghai Institute of Laser Plasma, China Academy of Engineering Physics, Shanghai 201800, China

Abstract

Objective High-efficiency broadband third-harmonic conversion is one of the key technologies of laser inertial confinement fusion driver. In the research of laser-driven inertial confinement fusion (ICF), neodymium glass laser frequency tripling (351 nm) is generally used to target to effectively improve the coupling efficiency of laser and plasma. At the same time, further increase the relative bandwidth ($\Delta\nu/\nu$) of the laser to $\sim 1\%$, which can effectively suppress the increase in instability during the interaction between the laser and the plasma, and reduce the generation of backward stimulated scattering and hot electrons. However, on account of high-speed optical field

modulation technology, narrow gain during high-gain amplification, and narrow high-efficiency frequency tripling bandwidth, the current output bandwidth of the laser driver is not greater than 0.3 nm (100 GHz). The broadband characteristics of super luminescent light and the wide, narrowband and frequency schemes provide a new way to realize this research.

Methods A numerical solution method for the harmonic conversion process under high power conditions is deduced. The necessity of studying super luminescent light is analyzed, and according to literature, a numerical model of super luminescent light is built, and combined with the numerical model of super luminescent light, the coupled wave equation for numerical simulation of the frequency tripling process of super luminescent light is given. The thickness of frequency doubling crystal and frequency tripling crystal is optimized to obtain the optimal solution under corresponding conditions. It also analyzes the evolution of the efficiency and spectral characteristics of the narrowband light with high time coherence as the sum frequency of the fundamental frequency light and the super luminescent light frequency doubled light. In addition, the direct frequency tripling process of super luminescent light, and the wide, narrowband sum frequency scheme of super luminescent light frequency doubled light and narrowband light input at different frequencies, and the wide, narrowband sum of super luminescent light fundamental frequency light and narrowband frequency doubled light are compared and analyzed. Frequency scheme. To judge the results of super luminescent light frequency tripling with different bandwidths, different wide, narrow bands and frequency schemes.

Results and Discussions Through simulation, it can be found that when the frequency doubling crystal is 19 mm, the fundamental frequency light intensity can obtain a more stable and efficient frequency doubling conversion efficiency in the range of 2-3 GW/cm². At this time, the frequency doubling conversion efficiency is $\sim 84.3\%$ (Fig. 3). Therefore, the ratio of the narrow-band fundamental frequency light energy to the super luminescent light pulse energy is set to 0.843: 2, which can make the ratio of the number of photons of the fundamental frequency to the frequency doubled in the sum frequency process close to 1:1. Choosing a 6 mm thick sum-frequency KDP crystal, the corresponding frequency tripling conversion efficiency can be as high as 44% (Fig. 3). By comparing the simulation results of the sum frequency of the broadband doubling frequency and the narrowband fundamental frequency and the direct frequency tripling (3 THz) of the super luminescent light pulse, it can be found that the introduction of narrowband can make the light intensity range 3-4 GW/cm². The maximum efficiency of the internal frequency tripling is increased from 5% to 44%. And its frequency tripling spectrum width is about 1.9 THz (Fig. 4). By comparing the wide, narrow and frequency processes of the super luminescent light input of different bandwidths, it is found that under the condition of 6 mm of the frequency tripling crystal thickness, the wideband fundamental frequency input of 2 THz and 1 THz can be fully converted over the entire spectrum. Obtain the frequency tripling spectrum waveform that is basically the same as the frequency doubling input, but as the bandwidth of the frequency doubling decreases, the bandwidth of the obtained frequency tripling will also decrease (Fig. 5). In addition, the super-radiation optical broadband fundamental frequency and narrow-band frequency multiplication and frequency schemes are compared, and it is found that the efficiency and spectrum results are consistent with the compensation for group velocity (Fig. 6).

Conclusions This paper establishes a numerical calculation model for the frequency tripling process of super luminescent light, simulates the frequency tripling process of super luminescent light frequency doubled light and narrow-band fundamental frequency light, and compares and analyzes the direct frequency tripling of super luminescent light and broadband super luminescent light frequency based. The frequency tripling and narrowband fundamental frequency optical sum frequency scheme proves that the wide, narrowband sum frequency scheme can effectively reduce the group velocity mismatch in the super luminescent light frequency tripling process, and theoretically can significantly improve the conversion efficiency and output. The frequency tripling bandwidth is close to 2 THz, and the conversion efficiency is greater than 40%, which is about 8 times higher than the direct frequency tripling efficiency of super luminescent light. This research provides theoretical guidance for the subsequent experiments to realize the broadband and efficient frequency tripling process of super luminescent light.

Key words nonlinear optics; super-luminescent light; nonlinear frequency conversion; group velocity mismatching

OCIS codes 190.2620; 190.4223; 350.2660